Visualization of Insulin-Loaded Nanocapsules: *In Vitro* and *in Vivo* Studies after Oral Administration to Rats

Huguette Pinto-Alphandary,[1,3] Malam Aboubakar,[1] Danielle Jaillard,[2] Patrick Couvreur,[1] and Christine Vauthier[1]

Received January 17, 2003; accepted April 2, 2003

Purpose. Biodegradable poly(isobutylcyanoacrylate) nanocapsules have been recognized as a promising carrier for oral administration of peptides and proteins. In the present study, we investigate the fate of insulin-loaded nanocapsules by fluorescence and transmission electron microscopy (TEM) after intragastric force-feeding to rats.

Methods. Insulin-, Texas-red®-labeled insulin, or gold-labeled insulin-loaded nanocapsules were first characterized. Rats received a single dose of nanocapsules (diameter 60–300 nm, 57 IU insulin/kg) by intragastric force-feeding. After 90 min, ileum was isolated and prepared for fluorescence and transmission electron microscopy.

Results. Nanocapsules were observed on both sides of the gut epithelium and in blood capillaries. In M-cell-free epithelium, apparently intact nanocapsules could be seen in the underlying tissue, suggesting they could cross the epithelium and carry the encapsulated peptide. In M-cell-containing epithelium, nanocapsules appeared degraded in the vicinity of macrophages. It is noteworthy that intestinal absorption of nanocapsules was observed without artifacts forcing the nanocapsules to stay in the gut.

Conclusions. Based on TEM observations, this study shows the intestinal absorption of biodegradable nanocapsules leading to the transport of insulin across the epithelium mucosa. The fate of the nanocapsules appeared different depending on the presence or the absence of M cells in the intestinal epithelium.

KEY WORDS: insulin; nanocapsules; poly(isobutylcyanoacrylate); oral delivery; intestinal tract.

INTRODUCTION

Proteins and peptides are very difficult to administer orally because of their susceptibility to enzymatic degradation in the gastrointestinal tract (1). To ensure the enteric protection of these molecules, various formulations have been developed. Microspheres (2,3) and microcapsules (4) have been described as more or less successful insulin carriers. However, numerous papers reporting the kinetics and mechanisms of the uptake and translocation of nano- and microparticles across the intestinal mucosa are contradictory (5). Nevertheless, three possible pathways for the absorption of drug carriers have been postulated (6,7): the first, via the M cells of the Peyer's patches; the second, via a transcellular route involving enterocytes; and last, via "paracellular avenues" through tight junctions (6). Various physicochemical factors seem to influence the translocation of particles across the epithelium, including the surface hydrophobicity, the nature of the polymer, and particle size (8). This last parameter certainly plays a key role in driving larger particles (3–10 μm) across the Peyer's patches (9–11), and smaller particles through the villus epithelium (10,12,13) before their transport into the bloodstream.

In previous studies, Lipiodol®-containing poly(isobutylcyanoacrylate) (PIBCA) nanocapsules intraluminally administered to dogs were found in the gut by scanning electron microscopy (14). They were located in close contact with mucus in intercellular spaces and in the mesenteric blood compartment. These insulin-loaded nanocapsules were shown to produce a dramatic reduction of the glycemia (50-60% by day 2; effect maintained for 20 days with a dose of 100 IU/kg) after intragastric administration to fasted streptozotocin-induced diabetic rats (15). The intensity and the duration of the effect were the most pronounced when the nanocapsules were administered in the ileum (16). These nanocapsules were also found efficacious in alloxan-induced diabetic dogs and capable of regulating other endocrine pancreatic dysfunctions: glucagonemia and somatostatinemia (17). These results strongly suggested that nanocapsules could deliver insulin directly to the blood (15–17). After intraduodenal administration of these insulin nanocapsules to rats, insulin could be detected in the blood at 30 min (18). Furthermore, Cournarie *et al.* (19) showed that after intragastric administration of the same insulin nanocapsules to rats, the peak of insulinemia appeared between 30 min and 1 h. Although there is a great variability depending on the rats, high rates of insulin could be detected in some rats (up to 250 mIU/L).

Further investigations on the stability of insulin-loaded nanocapsules (20) to enzymatic degradation (21) have shown them to have excellent resistance in gastric medium and poor stability in the intestinal medium. Also, Michel *et al.* (16) have shown a maximum effect after administration of the nanocapsules in the ileum, suggesting that insulin nanocapsules could preferentially be absorbed by this part of the intestine. However, the gut cells involved in nanocapsule translocation remain completely unknown. Thus, the aim of the present study was to investigate this point using both fluorescence microscopy and transmission electron microscopy. Transmission electron microscopy (TEM) was used here in combination with fluorescence microscopy to reach a high level of resolution allowing the identification of single nanocapsules in the intestinal tissue. In this study, the nanocapsules were administered to normal rats, following a protocol respecting physiologic conditions and consisting in one single administration as suggested by Jani *et al.* (12). This constitutes an original approach considering many studies based on nonphysiologic models including every day force-feeding (10), *in situ* loop model (22), *in vivo* isolated intestinal segments (14,23,24), and *in situ* intraluminal deposition (25).

MATERIALS AND METHODS

Materials

Isobutylcyanoacrylate (IBCA) was a gift from Loctite (Ireland), Lutrol® F68 (Poloxamer® 188) was kindly provided

[1] UMR CNRS 8612, Laboratoire de Physico-Chimie, Pharmacotechnie et Biopharmacie, Faculté de Pharmacie, Université Paris XI, 92296 Châtenay-Malabry Cédex, France.

[2] UPRES-A CNRS 8080, Service Commun de Microscopie Électronique, Université Paris-Sud, 91405 Orsay Cédex, France.

[3] To whom correspondence should be addressed. (e-mail: Huguette.Alphandary@cep.u-psud.fr)

by BASF (Germany), and Miglyol® 812N by Lambert Riviere (France). Glutaraldehyde was purchased from Sigma (France), osmium tetroxide (OsO_4) from Comptoir Lyon Alemand Louyot (France), and ethanol from Carlo Erba (Italy). Epon- and Formvar-coated grids (Fullam) were obtained from Touzart et Matignon (France). Sodium cacodylate, phosphotungstic acid, uranyl acetate, and lead citrate were obtained from Merck-Eurolab (France). Texas Red® succinimidyl ester was supplied by Molecular Probes (Leiden, The Netherlands).

Insulin (INS) and gold-labeled insulin (AuINS) were supplied by Sigma (France). According to the supplier specifications, particle size of colloidal gold was 8–12 nm in diameter. Texas red®-labeled insulin (INS-TR) was prepared as described elsewhere (21).

Methods

Insulin-Loaded Nanocapsules

Insulin-loaded nanocapsules (INS-NC) were prepared by interfacial polymerization of IBCA as previously described (15,20). Briefly, insulin (5 mg) was added to 25 ml of absolute ethanol containing 1 ml of Miglyol® 812N and 125 μl of IBCA. This organic phase was added under magnetic stirring to 50 ml of an aqueous solution of Lutrol® F68 (0.25%). The resulting suspension of nanocapsules was concentrated by rotoevaporation to a final volume of 10 ml. This method allows quantitative encapsulation of insulin (15,16,18,26). The insulin content was 500 μg/ml, and the encapsulation yield was 100% as determined by HPLC (20). Zeta potential measurements (26) showed that insulin was mainly located inside the nanocapsules.

Texas Red®-Labeled Insulin-Loaded Nanocapsules

Texas red®-labeled insulin-loaded nanocapsules (INS-TR-NC) were prepared as described above, except that INS-TR was used instead of insulin. INS-TR-NC were purified by chromatograpy on Sephadex® G-50 as explained elsewhere (21).

Gold-Labeled Insulin-Loaded Nanocapsules

Gold-labeled insulin nanocapsules (AuINS-NC) were prepared as described above, except that gold-labeled insulin was used instead of insulin. The suspension of AuINS-NC was ultracentrifuged at 112,000 *g* for 2 h at 4°C (Beckman model L7-55 ultracentrifuge, Beckman Instruments, France) to remove free AuINS and then resuspended in physiologic saline solution. The insulin content was 500 μg/ml as in INS-NC.

Stability of the Nanocapsules in Reconstituted Intestinal Medium

Insulin-loaded nanocapsules were incubated for 5 h in reconstituted intestinal medium (USP XXIII) at 37°C before observations by TEM.

Animal Experiments

Male Wistar adult rats (average weight 350 g) were fasted overnight, and 2 ml of INS-NC, INS-TR-NC, or AuINS-NC suspension (10 IU insulin/ml; i.e., 0.5 mg/ml; i.e., 2.8 mg/kg) were administered intragastrically to two, two, and three animals, respectively. Control rats ($n = 2$) received a control solution of INS, INS-TR, or AuINS in 0.9% sodium chloride (2 ml). Tissues for fluorescence microscopy or TEM were isolated after 90 min of treatment. Indeed, according to Aboubakar *et al.* (21), insulin nanocapsules were found in the ileum after 1 or 2 h after administration. This also corresponds to the absorption peak of insulin given as nanocapsules by the oral route (19). The research adhered to the "Principles of Laboratory Animal Care" (NIH publication #85-23, revised 1985).

Transmission Electron Microscopy

Formvar-coated grids were ionized under UV light exposure (220 J). INS-NC, AuINS-NC, or INS-NC incubated in reconstituted intestinal medium were loaded by floating the grids, which were then either left unstained or negatively stained with 2% uranyl acetate. Observations were made with an electron microscope JEM 1200EX (JEOL, France) operating at 80 kV.

To prepare ultrathin sections, the AuINS-NC and gold-labeled insulin used as controls were suspended in 2.5% agar at 45°C (v/v). The mixture was rapidly shaken and cooled using an ice bath. The resulting gel blocks were cut into small pieces and placed in buffer A (0.4 M phosphate, pH 7.3, 0.1 M saccharose) at 20°C. Samples were fixed with 1% glutaraldehyde in buffer A for 15 min and washed with buffer A. Samples were then postfixed with 1% OsO_4 in buffer B (0.2 M phosphate, pH 7.3) for 15 min and washed with buffer B. The samples were dehydrated through a graded series of ethanol solutions and embedded in Epon. The embedded material was cut into ultrathin sections (70–90 nm) (Ultracut UCT, Leica, France) and loaded on grids before being stained with 2% uranyl acetate (10 min) or double-stained with 2% uranyl acetate (20 min) and then with 0.2% lead citrate (10 min) (classic double staining). Grids were observed with a transmission electron microscope (EM208, Philips, France) operating at 80 kV.

For tissue preparation, 90 min after the administration of the samples, control and treated animals were anesthetized by a pentobarbital injection and subsequently intracardiacally perfused with the Ringer's liquid (100 ml) and with the Wuerker's fixative (500 ml). The ileum was removed and fixed for 2 h. The tissues were washed in phosphate buffer pH 7.4, cut in small pieces, and postfixed with 1% OsO_4 containing 0.2 M cacodylate buffer pH 7.4, for 2 h. The samples were washed in 0.1 M cacodylate buffer, dehydrated through graded series of ethanol solutions, and embedded in Epon. Ultrathin sections were collected on grids and left unstained or were stained as described above. In the case of AuINS-NC, the staining time was reduced to avoid artifacts. Examinations were performed as described above.

Fluorescence Microscopy and Confocal Laser Scanning Microscopy

INS-TR solution or INS-TR-NC were intragastrically administered to fasted rats. The animals were sacrificed after 90 min. Portions of the small intestine were embedded in cryo-

stat medium Tissue-Tek® (Miles, USA). Thin sections (5 μm) made using a Cryomin® (OSI, Maurepas, France) were mounted in AF1 solution (Cityfluor Ltd., England). Fluorescent microscopy was performed using a fluorescent microscope (Leitz Diaplan, Leica, Rueil-Malmaison, France) equipped with a filter adapted to Texas-red® (λ excitation 515–561 nm, λ emission cutoff 590 nm). For confocal microscopy, the optical sectioning was performed with an MRC1024 Microscope (Bio-Rad, Ivry, France) equipped with a krypton-argon-ion laser using the 568-nm line.

RESULTS

TEM Observations of INS-NC and AuINS-NC

Under TEM, insulin-loaded nanocapsules were visualized as particles with a size ranging from 60 to 250 nm (Fig. 1). Figures 1 and 2 show representative magnifications of the nanocapsules, the structures of which appeared to be unaffected by the TEM sample preparation process. With the unstained nanocapsules, an electron-dense core with an electron-transparent envelope could be seen (Fig. 1a,c). The core of AuINS-NC appeared much more opaque to electrons than that of INS-NC. A very thin electron-dense layer delimited the envelope. Staining INS-NC with uranyl acetate did not modify the general appearance of the nanocapsules (Fig. 1b), and their apparently heterogeneous aspect could be caused by the superimposition of several nanocapsules.

Figure 1d shows the appearance of nanocapsules incubated 5 h in the reconstituted intestinal medium. Rings and polymeric-like material were observed.

Because the intestinal tissue was embedded in Epon and observed as ultrathin sections, AuINS-NC and AuINS were treated in the same conditions. So, the nanocapsule structure in ultrathin sections was more clearly defined than those of INS-NC (Fig. 2). Stained preparations (Fig. 2b,c) showed a cavity filled with material highly opaque to electrons, compared to the unstained preparations (Fig. 2a). Indeed, in the unstained ultrathin sections, the contrast of the nanocapsules depended on the thickness of the nanocapsules, taking into account the ultracutting plan. The envelope appeared about 10 nm thick. Colloidal gold grains from AuINS shown in Fig.

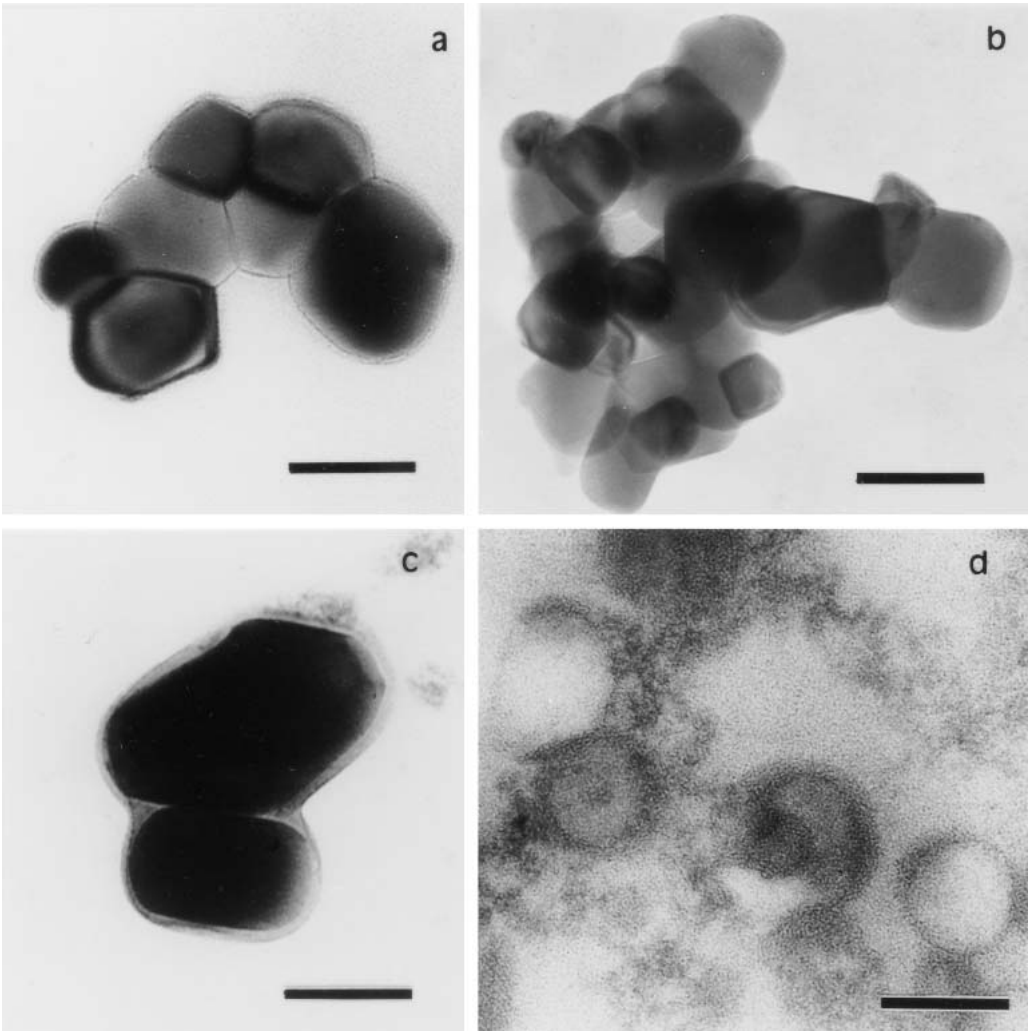

Fig. 1. Direct observation of insulin-loaded nanocapsules by TEM. INS-NC without staining (a), stained with uranyl acetate (b); AuINS-NC without staining (c); INS-NC after 5-h incubation in reconstituted intestinal medium; stained with uranyl acetate; ring forms and surrounding polymeric material (d). Bar represents 100 nm.

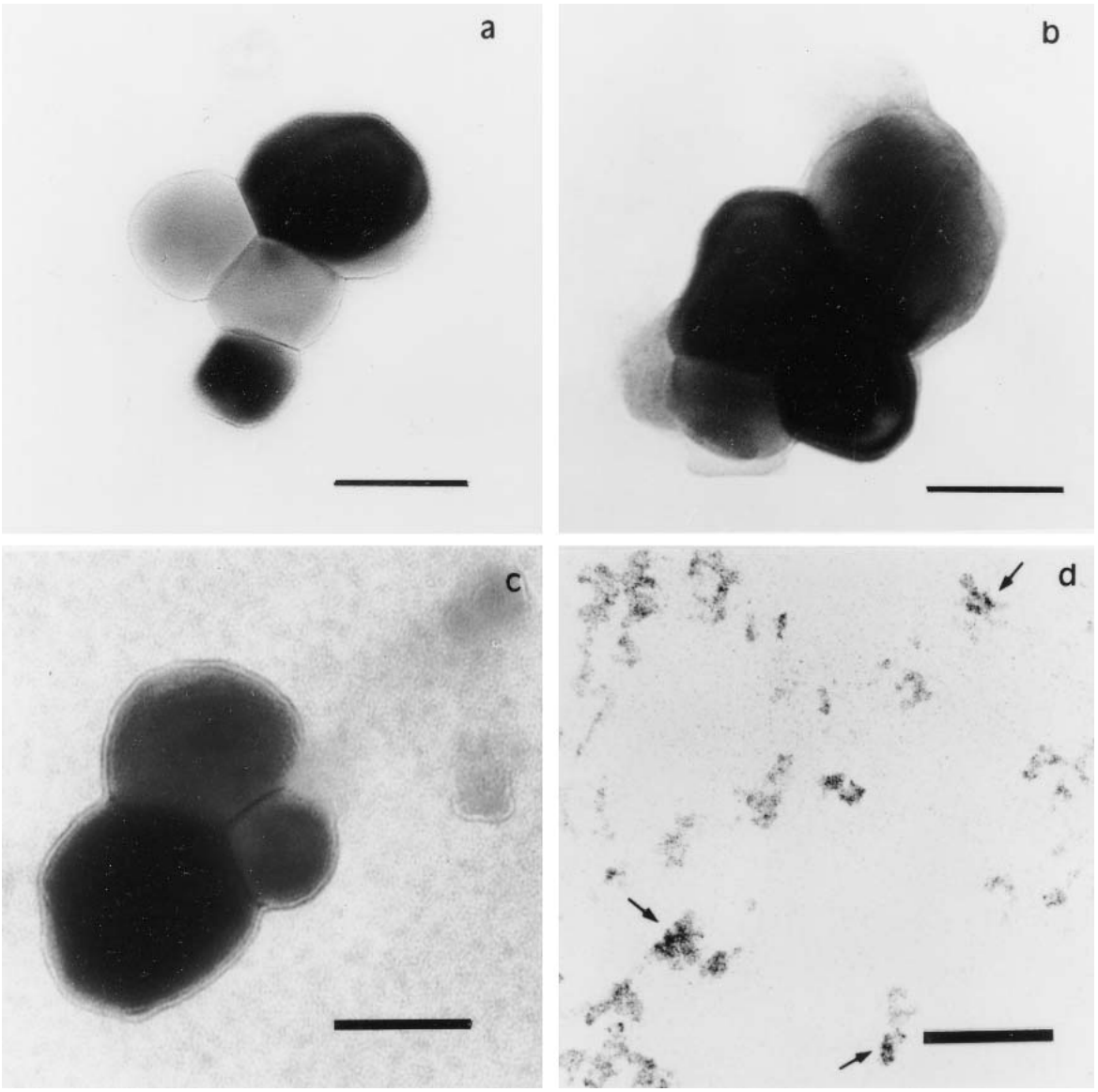

Fig. 2. Ultrathin sections of AuINS-NC without staining (a), stained with uranyl acetate (b), and double-stained (c). Gold-labeled insulin used as control (d); arrows indicated gold particles. Bar represents 100 nm.

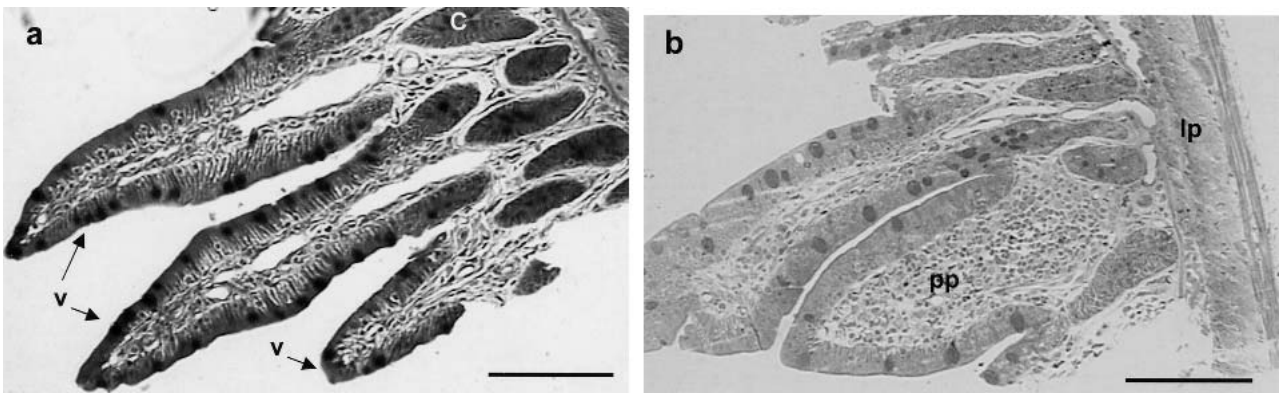

Fig. 3. Semithin section (5 μm) stained with methylene blue for the localization of areas observed by TEM. (a) region of M-cell-free epithelium, c, crypt, v, intestinal villa; (b) region of M-cell-containing epithelium, lp, lamina propria, pp, Peyer's patch. Bars represent 100 μm.

2d were readily identified; however, they appeared smaller, 4–5 nm, than the size given by the supplier, 8-12 nm.

TEM Observations of INS-NC in the Intestinal Tissue

The figures presented in this report corresponded to relevant observations of nanocapsules made on most of the examined samples. For each animal, hundreds of ultrathin sections were examined by TEM in order to identify the nanocapsules. Different areas of the gut of rats treated with oral INS-NC were examined (Fig. 3, a semithin section). In Fig. 4, ultrathin sections showed particles with a general aspect similar to that of the nanocapsules shown in Fig. 2. Large clusters of nanocapsules with diameters of ~50 nm were found in the lumen (Fig. 4a,c), whereas smaller groups of nanocapsules could be seen on the brush border of enterocytes in close contact with the glycocalyx filaments (Fig. 4b,c). Other sections (data not shown) contained nanocapsules in various sites of the intestinal epithelium: enterocytes, goblet cells,

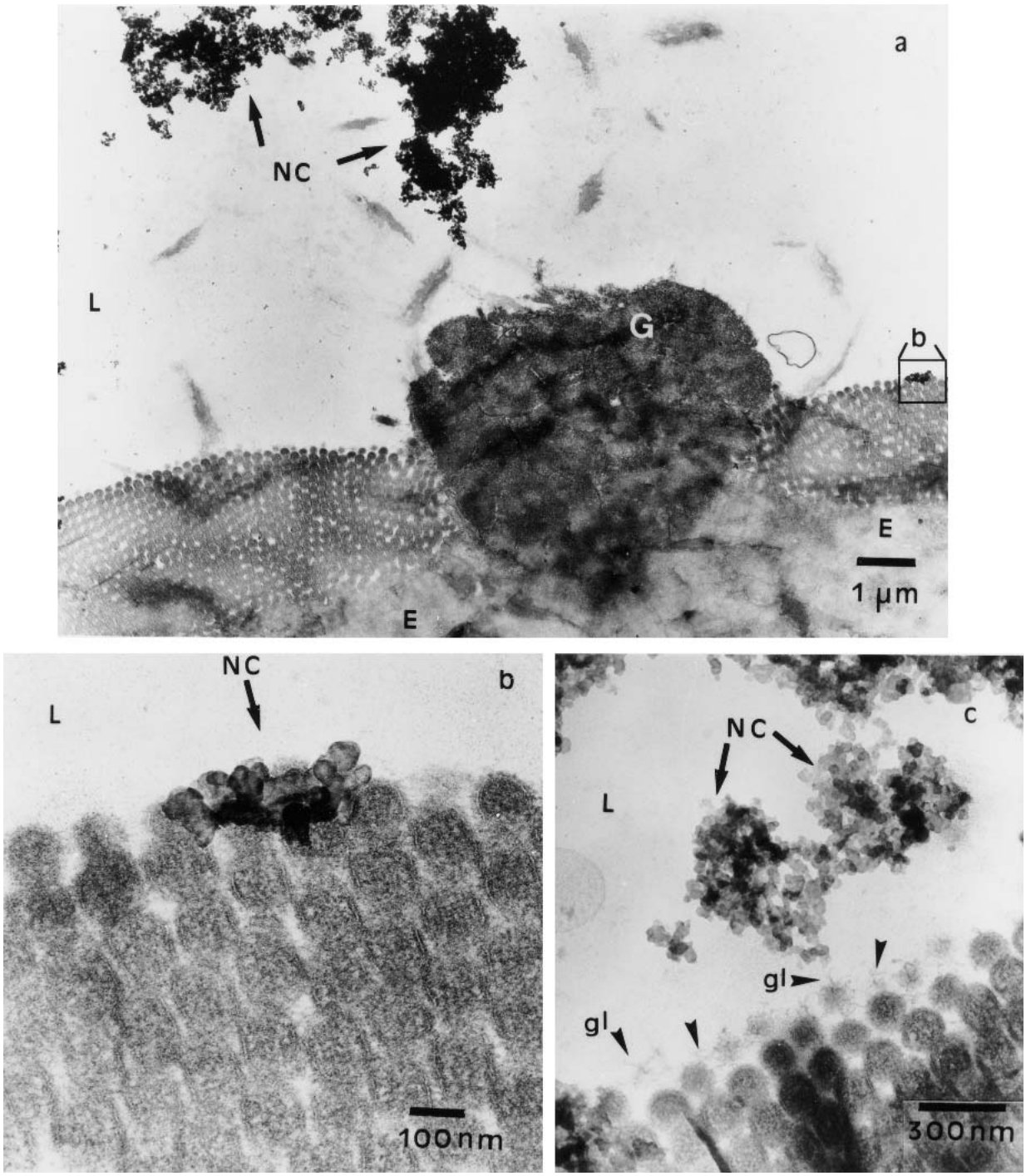

Fig. 4. Electron micrographs of ultrathin sections (classic staining) of ileum isolated from rats after intragastric administration of INS-NC. (a) NC in the lumen (L); large clusters above a goblet cell (G) surrounded by enterocytes (E). (b) Nanocapsules (NC, arrows) adherent to the enterocyte microvilli (detail of a). (c) Magnification of an area at the right side of (a) showing nanocapsules (NC, arrows) close to the microvilli with glycocalyx filaments (gl, arrowheads).

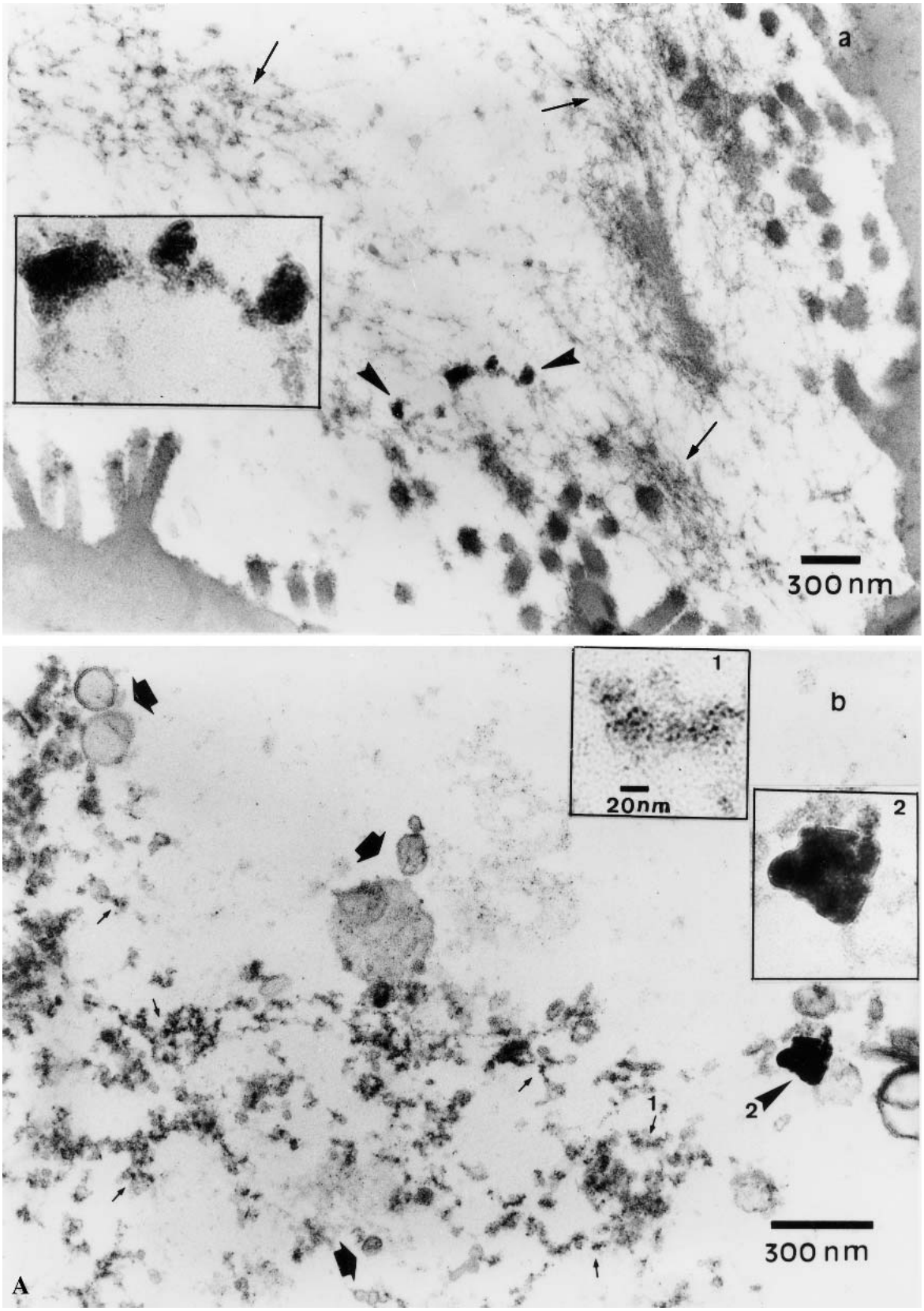

Fig. 5. Electron micrographs of ultrathin sections of ileum isolated from rats after intragastric administration of AuINS-NC. Staining: uranyl acetate (10 min) and lead citrate (2 min). A non-M-cell-containing region. (A) Bottom of a crypt in the lumen side. (a): NC (arrowheads) in the process of degradation associated with polymeric material and gold particles (arrows); magnification more than 3×. (b) NC (arrowhead) and gold particles (arrows) associated with polymeric material and ring structures (thick arrows), and detail of areas noted 1 and 2. (B) Underlying tissue: (a) clusters of NC (a magnification in the squared area) and a string of NC in a blood capillary (BC), magnified in (b); (c) typical aspect of NC in a blood capillary with dark NC (arrowheads) and ring forms (arrows); (d) another cluster of NC.

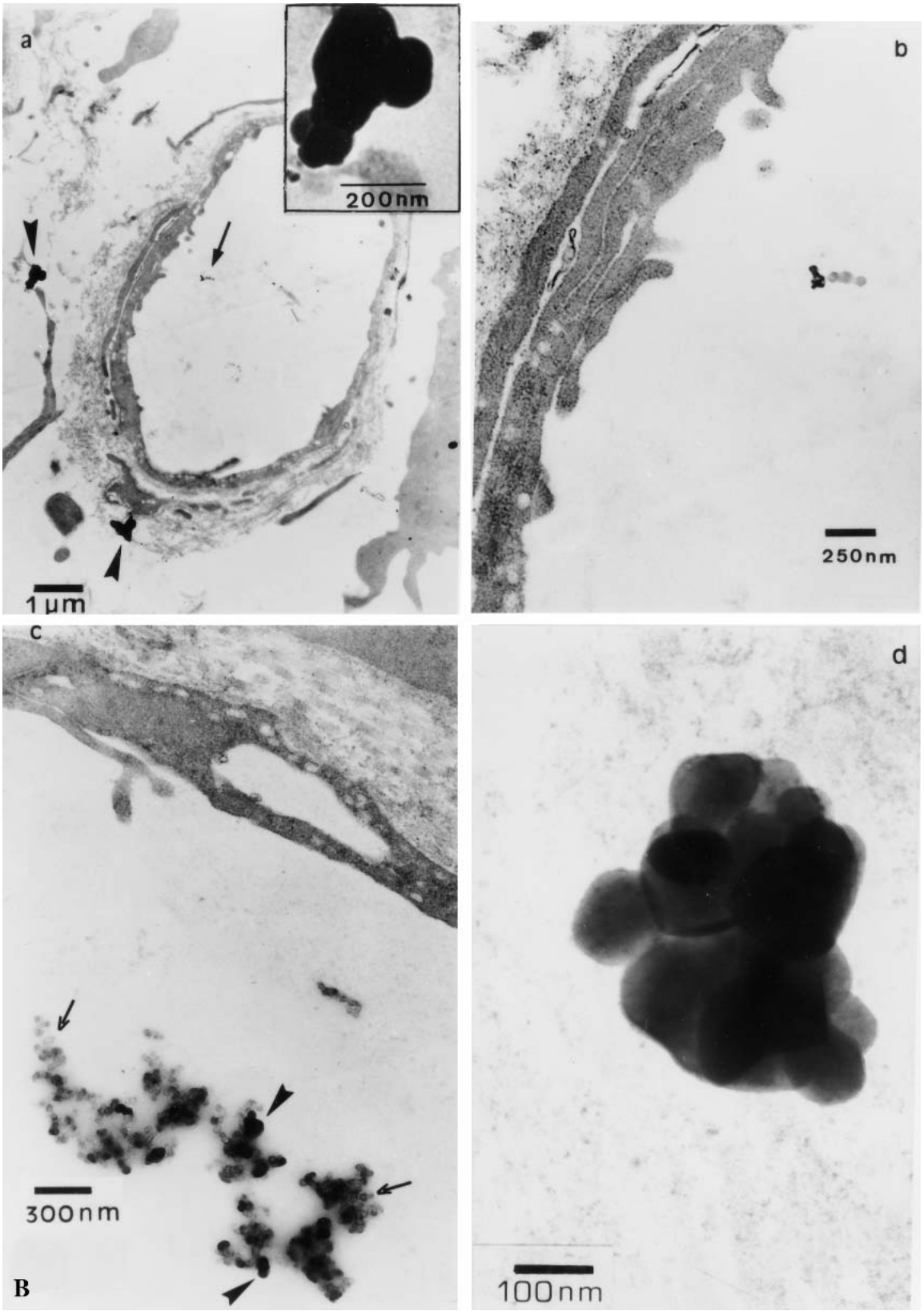

Fig. 5B.

intercellular spaces, muscular layer, conjunctive tissue, and blood capillaries.

TEM Observations of AuINS-NC in the Intestinal Tissue

Different areas of the gut of rats that received AuINS-NC were examined. Nanocapsules accumulated in the intestinal crypts (Fig. 5A, arrowheads), and some appeared with an apparently intact wall less electron-dense than the core (Fig. 5Ab). Some others seemed to release their content (Fig. 5Aa,b). Some others appeared more degraded with a ring-like form (Fig. 5Ab, arrows). All of these structures were surrounded by material with a typical polymeric appearance (Fig. 5Aa,b) showing many dark grains, the size of which corresponded to that of the colloidal gold particles used as an insulin marker (Fig. 5Aa,b, arrows): 4–5 nm as in the control (Fig. 2d). Clusters of nanocapsules (Fig. 5B) could be seen in many places in the underlying tissue. As a rare event, some nanocapsules could be seen in blood capillaries (Fig. 5Ba–c).

Figure 6 shows a region with phagocytic cells including lymphocytes (Fig. 6a) in the intraepithelial "pocket" of M cells. Some polymeric material was seen in intercellular spaces formed by the interpenetrating pseudopods of the phagocytic cells (Fig. 6a–c). This extensively degraded material (Fig. 6c, arrows) contained numerous gold particles (Fig. 6d) similar to those observed in the crypt (Fig. 5B).

Figure 7 shows the ultrastructure of the control tissue after classic double staining. An enterocyte with its brush border is shown in Fig. 7a. Figure 7b displays well-preserved mitochondria and ribosomes. Ribosomes were observed to have a diameter of ~30 nm, a granular appearance, and an indistinct outline. Some dense structures (c) and granules (d)

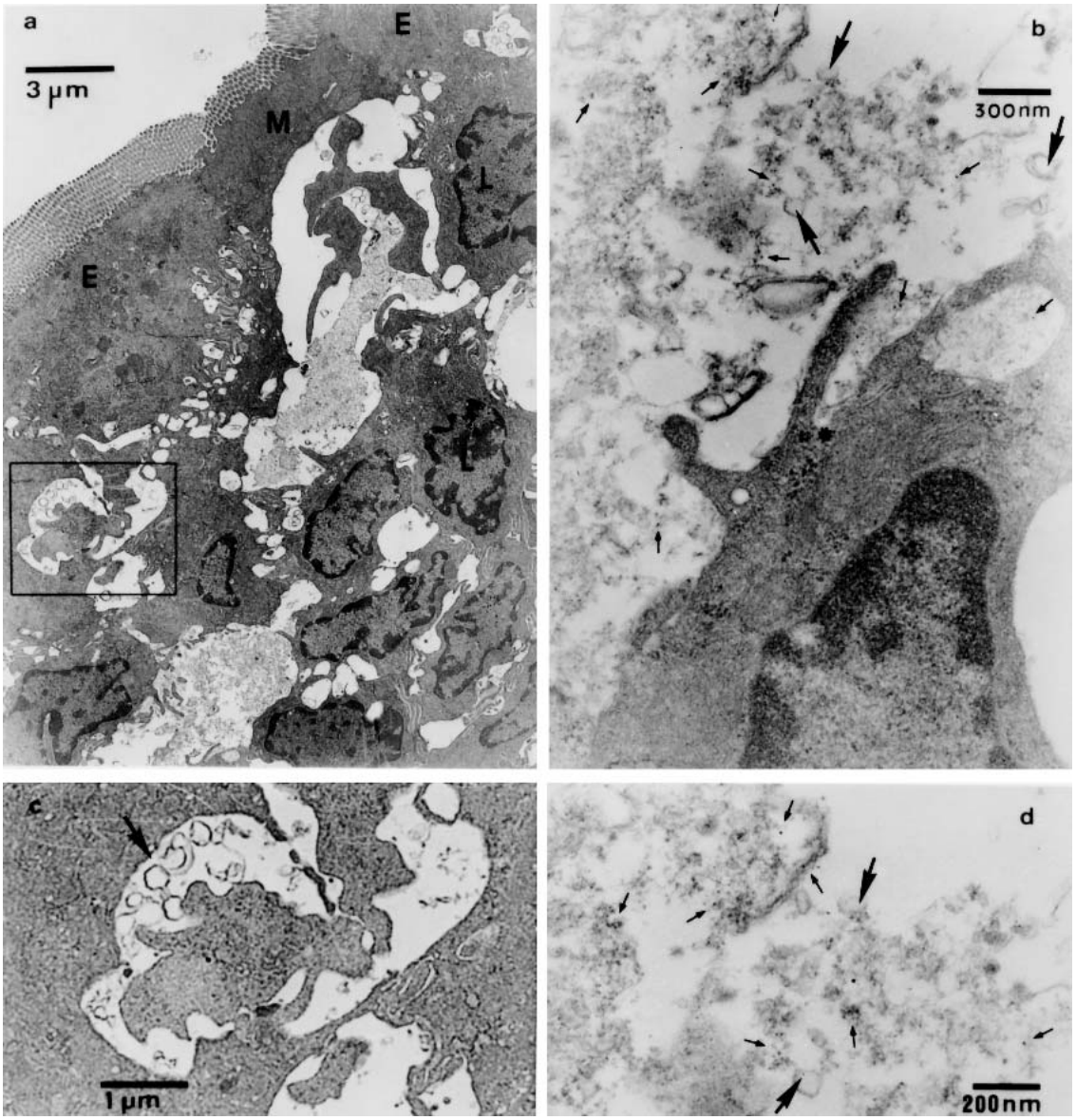

Fig. 6. AuINS-NC in an M-cell region. E, enterocyte; M, M cell; L, lymphocyte. Staining: uranyl acetate (10 min). (a) General view showing ring forms and very degraded material in vacuoles; (b) detail of the area adjacent to the bottom of (a) showing the numerous gold particles (short arrows) and the ring forms (arrows) in the intraepithelial "pocket." Ribosomes are indicated with an asterisk. (c) and (d) are details of (a) and (b), respectively, showing ring forms (arrows) and gold particles (short arrows).

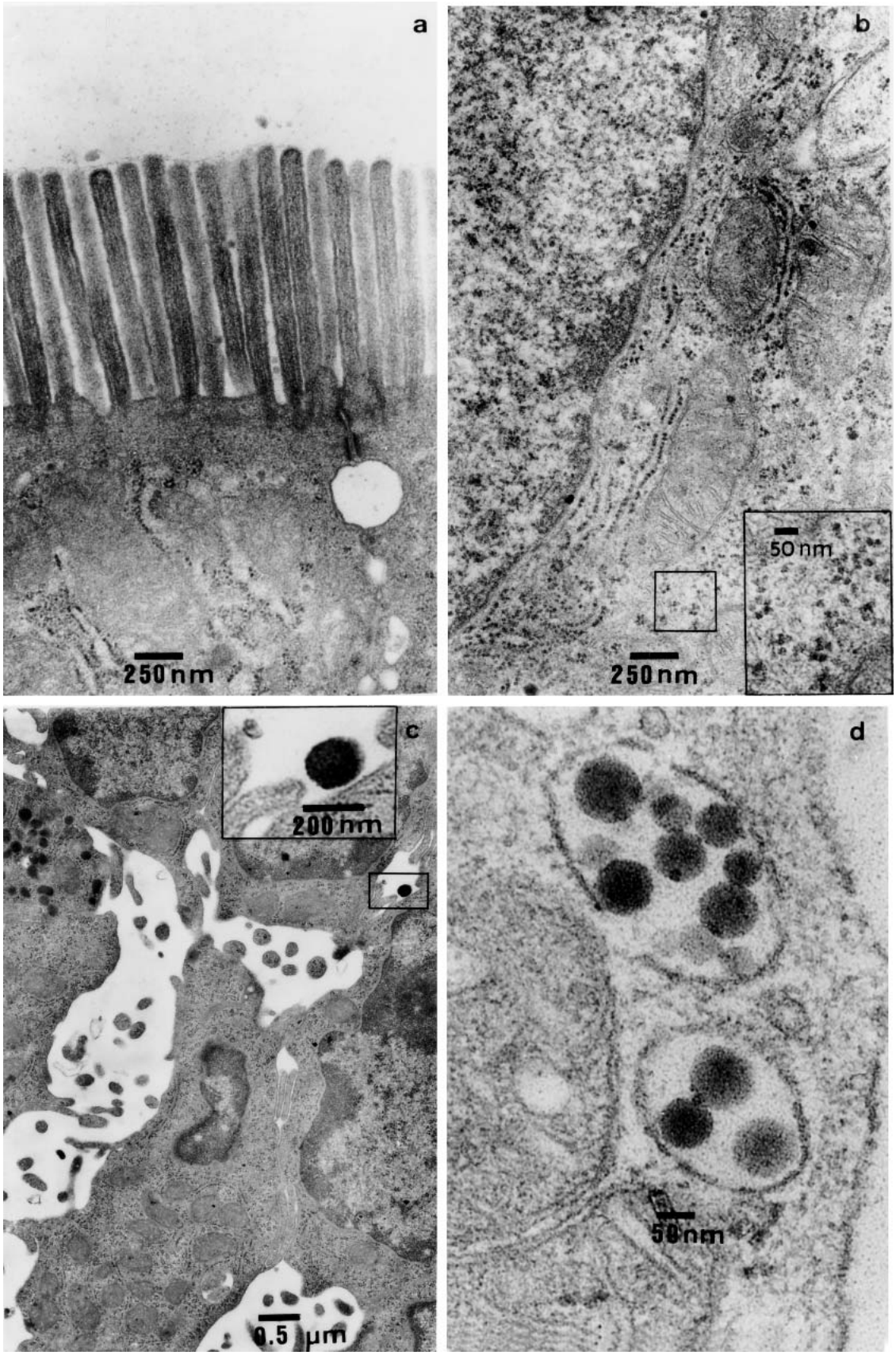

Fig. 7. Electron micrographs of ultrathin sections of ileum isolated from control rats. The sections are classically double stained. (a) enterocyte; (b) mitochondria and ribosomes; the squared area is magnified, and ribosomes are indicated by an arrow; (c) intercellular spaces in the underlying tissue; the magnified area shows material with a granulous aspect; (d) granules in the intestinal tissue (arrowhead).

were magnified to show their different appearance compared to that of the nanocapsules. In any case, examinations carried out on control tissues (Fig. 7) did not reveal any structure similar to that of nanocapsules observed in Figs. 1 and 2.

Fluorescence Microscopy and Confocal Microscopy Observations

Sections of ileum of rats fed with INS-TR-NC showed different patterns depending on the observed epithelium portion and more precisely on the absence (Fig. 8b,c) or the presence of Peyer's Patches (Fig. 9b). In the absence of M cells, zones with intense fluorescence could be located inside the villi (Fig. 8b). Confocal microscopy of a villus revealed many small spots of fluorescence (Fig. 8c). In Peyer's patches, diffuse fluorescence appeared in the subjacent epithelial tissue (Fig. 9b). Sections of the ileum of rats treated with a single solution of INS-TR are presented in Figs. 8a and 9a. No fluorescence could be detected in the villi (Fig. 8a), whereas only very light spots of fluorescence corresponding to the nucleus of certain cells appeared in Peyer's patches (Fig. 9a).

DISCUSSION

This study visualizes the fate of insulin nanocapsules in the ileum of rats after a single intragastric administration performed under physiologic conditions. In previous reports, the main site of absorption for the insulin-loaded nanocapsules was shown to be the ileum (16); thus, only this segment was considered in the present study. Intestinal tissue contains a number of structures that may be mistaken for nanocapsules when observed with microscopy techniques, thus making clear identification difficult (3,7). Insulin-loaded nanocapsules were therefore carefully characterized by TEM in order to facilitate their detection in the intestinal tissue. Gold-labeled insulin was used as a marker of the encapsulated insulin to improve the contrast in TEM. Fluorescence and confocal microscopy were used as additional lower-resolution

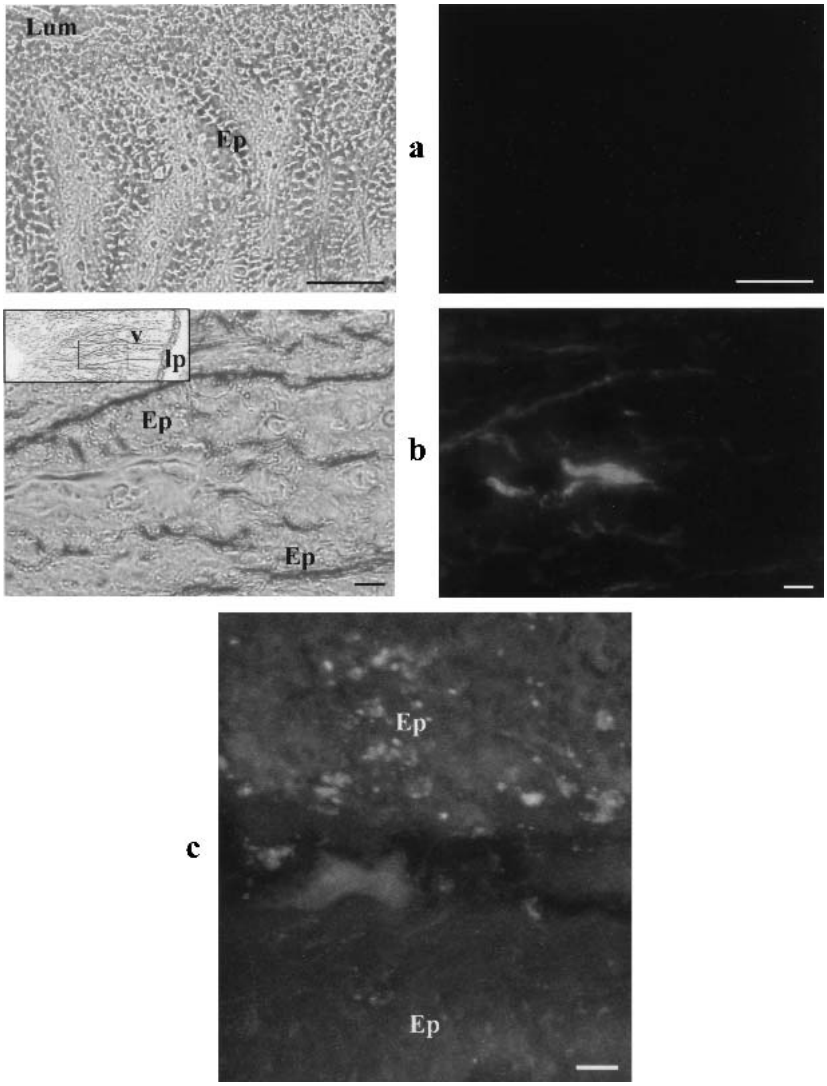

Fig. 8. Fluorescence microscopy and confocal microscopy in the small intestine tissue after administration of INS-TR-NC. Left side, normal mode; right side, fluorescent mode. (a) Control villi (INS-TR); (b) INS-TR-NC in the villi; (c) confocal micrograph INS-TR-NC in a villus. The bar represents 100 μm (a) and 10 μm (b,c). Ep, epithelium; lp, lamina propria; Lum, lumen; v, villus.

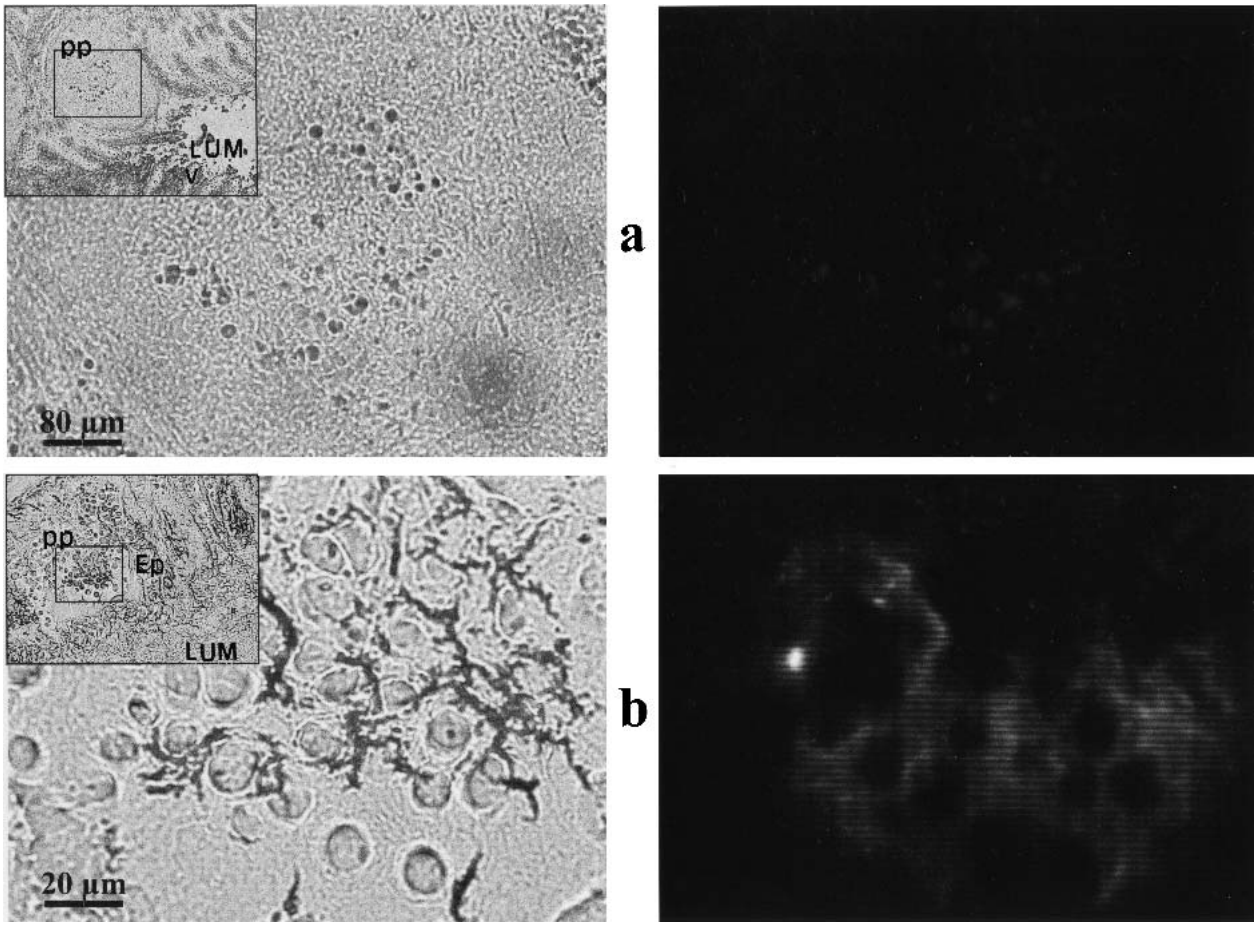

Fig. 9. Fluorescence microscopy in the small intestine tissue after administration of INS-TR-NC. (a) Control Peyer's patch (INS-TR); (b) INS-TR-NC in Peyer's patch. The bar represents 80 µm (a) and 20 µm (b). pp, Peyer's patch.

techniques to provide a general overview of the fate of insulin-loaded nanocapsules.

TEM observations of insulin-loaded nanocapsules clearly showed the vesicular structure of the particles with a cavity filled with an electron-dense material, especially when Au-INS was used (Figs. 1c, 2b,c compared to Fig. 1a,b). Nanocapsule envelope surrounding the oily core was limited by an external thin layer of electron-dense material that could correspond to Poloxamer® 188 or, alternatively, to a small amount of insulin adsorbed onto nanocapsule surface. The further enhancement of the contrast of the oily core by heavy metals emphasized the fact that insulin was located inside the nanocapsule core, as previously suggested (20). Indeed, OsO_4 promoting the electron contrast is known to react with amino-acid residues present in insulin (His, Lys, Cys). Both methods of nanocapsule preparations (deposit and inclusion) led to identical features in a reproducible fashion. These results show that the method used here to prepare specimens for TEM preserved the integrity of the nanocapsules and that the general aspect of the nanocapsules was not affected by TEM preparations.

In the intestinal tissue, INS-NC could be clearly seen and distinguished from cellular material (Fig. 4). The aspect of nanocapsules found in crypts was somewhat different than *in vitro* because of the degradation process. Depending on the area observed, they appeared either with a similar morphology (Figs. 5Ab and 5Ba,d) as nanocapsules alone (Fig. 2a–c), or as rings with a light core delimited by a dark wall (Figs. 5Ab, 5Bc, and 6) and surrounded by polymeric material and gold particles (Figs. 5A and 6b,d). Intermediate forms could be seen in the process of degradation (Fig. 5Aa). The ring form could correspond to highly degraded nanocapsules compared to Fig. 1d and in agreement with a previous report (27). The use of AuINS facilitated the identification of nanocapsules in tissue sections. Gold particles with a regular size of about 4–5 nm in diameter and a distinct outline (Fig. 2d control, Fig. 5Ab detail 1, Fig. 6b,d) were clearly identified and could not be mistaken for ribosomes, which are ~30 nm in diameter with a granular appearance and indistinct outline (Fig. 6b, Fig. 7b control) or with granules of intestinal cells (Fig. 7c,d).

Nanocapsules were widely dispersed in the intestinal tissue, on both sides of the epithelium. In the lumen, apparently intact nanocapsules appeared as quite large clusters close to the top of goblet cells, suggesting that they were more or less embedded in mucus (Fig. 4a,b) or interacting with the glycocalyx of enterocytes (Fig. 4c). At this level, insulin located in the nanocapsule cavity could be protected against enzymatic degradation. Indeed, a protective role of the mucus against polymer degradation was pointed out *in vitro* for PIBCA nanospheres (28). The tendency of the nanocapsules to form clusters *in vivo* has already been mentioned for various nanoparticulate carriers (29). Cluster formation may be attributed to some bioadhesive properties of the nanocapsules because

of their polymer envelope and the presence of Poloxamer® 188, which was shown elsewhere to modulate the bioadhesion of particles onto the intestinal mucous membrane (30). The gold colloidal particles seen in the lumen side of the crypts could be the signature of a release of gold-labeled insulin from partly degraded nanocapsules. Because the amount of mucus is reduced in crypts, nanocapsules may therefore be more sensitive to degradation. This is in agreement with previous experiments performed *in vitro* in the absence of mucus, showing that nanocapsules became leaky in the presence of intestinal enzymes (21).

Nanocapsules were also observed in the underlying tissue, indicating they could cross the epithelium. The appearance of the nanocapsules was different whether they were observed under the epithelium free from M cells or under the M-cell-containing epithelium. Indeed, in the first case, nanocapsules found in the space between the enterocyte basolateral side and the blood and lymphatic vessels showed a diameter lower than 150 nm. The nanocapsules appeared to be much more like intact nanocapsules regarding the clearly degraded nanocapsules observed in crypts (Fig. 5A) and in the regions containing M cells (Fig. 6). By fluorescence and confocal microscopy, this appeared as bright concentrated spots of fluorescence in the intestine of rats that received INS-TR-NC. This suggests that insulin was still trapped in the nanocapsules, even after intragastric administration and intestinal absorption. This strongly supports the suggestion that insulin could be protected by nanoencapsulation and further transported across the epithelium to reach the blood circulation. The translocation appeared to be limited to nanocapsules with a maximum diameter of 150 nm in agreement with previous reports considering other types of particles (6,10,31).

In regions located under the M-cell-containing epithelium, the nanocapsules had the appearance of rings surrounded by an electron-dense material showing gold particles (Fig. 6). The polymer forming the nanocapsule envelope appeared partly degraded, and the free gold particles indicated a massive release of insulin. By fluorescence microscopy, the diffuse fluorescence observed in the subjacent tissue in the Peyer's patch of rats that received INS-TR-NC suggested that the fluorescent insulin was released from the nanocapsules and diffused into the surrounding tissue. These data are in agreement with an increased esterase activity that has been described along the M-cell apical side (32) and that may be responsible for the degradation of the polymer. Poly(isobutylcyanoacrylate) present in the nanocapsule envelope is well known to be degraded by esterases (33). It should be noted that once released under these conditions, the insulin was no longer protected from enzymatic attack.

The rate of nanocapsule uptake was difficult to estimate, but it could be considered to be low when compared to the large clusters of nanocapsules observed by TEM in the intestinal lumen (Fig. 4). In addition, because of the extensive fixative perfusion of rats during preparation of tissues for TEM, the major part of nanocapsules could be washed from blood capillaries. Because only some aggregates remained adherent, the rate of nanocapsule uptake was underestimated. No specific mechanism of transport of the nanocapsules through the intestinal epithelium could be identified because nanocapsules were located in enterocytes, goblet cells, and intercellular spaces before they reached the blood capillaries (Figs. 4 and 5). However, this transport was found to be limited in M-cell-free epithelium portions to intact nanocapsules with a maximum diameter of 150 nm. Therefore, the nano-

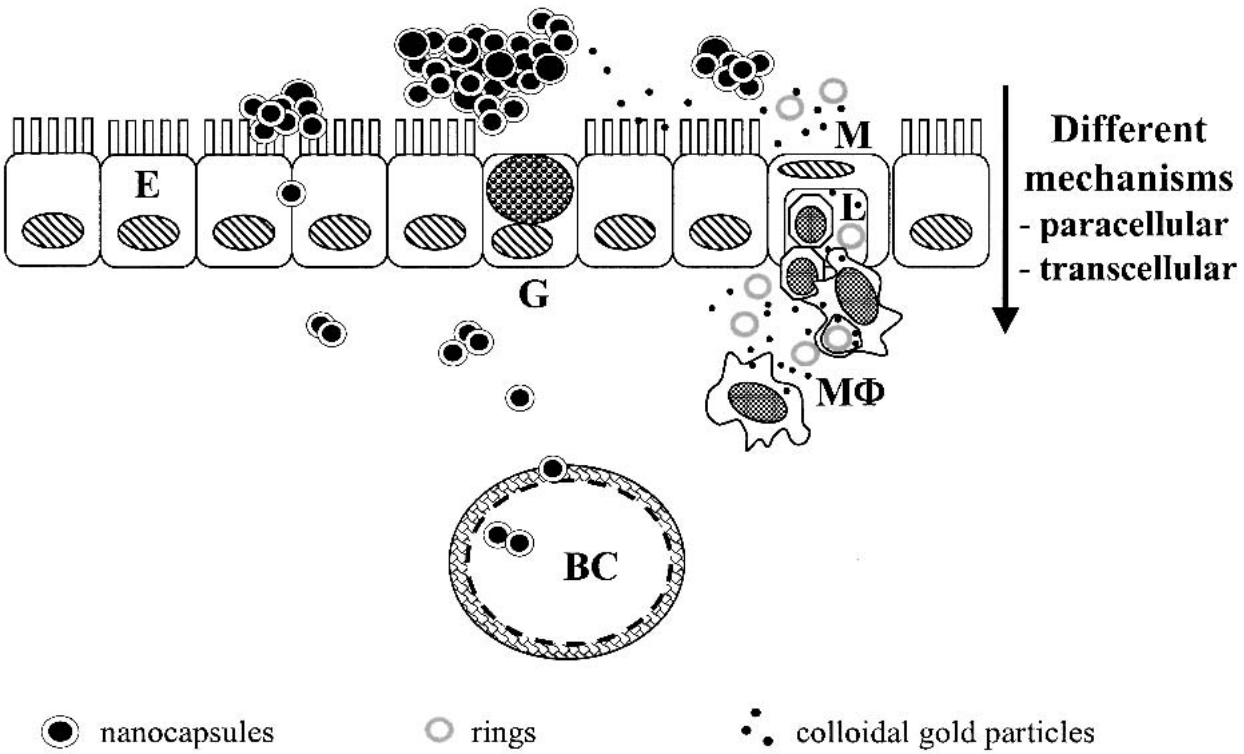

Fig. 10. Model of *in vivo* fate of the insulin-loaded nanocapsules in the ileum after intragastric administration. BC, blood capillary; E, enterocyte; G, goblet cell; L, lymphocyte; M, M cell; MΦ, macrophage.

capsules could penetrate into blood capillaries (Fig. 5B) through the fenestrations of their basement membrane, which generally have diameters from 500 nm to 5 μm (29). On reaching the blood circulation, the nanocapsules may be degraded by serum esterases (33), releasing insulin into the blood. This can explain the systemic delivery of insulin reported by Lowe and Temple (18) and Cournarie *et al.* (19). As already suggested before for other types of nanoparticles (3,12,14,21,34), this study showed that different mechanisms coexist to allow insulin-loaded nanocapsules to be absorbed by the intestinal epithelium. However, because of the biodegradable nature of the polymer forming the nanocapsule envelope, different fates of the nanocapsules could be highlighted depending on the structure of the absorptive portion of the epithelium as illustrated in the model proposed in Fig. 10. Beside the passage of nanocapsules through the epithelium as illustrated in Fig. 10, other ways of absorption may be proposed to explain the good bioavailability reported elsewhere of insulin by the oral route using these nanocapsules. Based on the observations of degraded nanocapsules in crypts, it could be suggested that the insulin released from nanocapsules in the vicinity of the gut cells may also be directly absorbed by the gut.

CONCLUSION

In conclusion, our data clearly demonstrated that nanocapsules could actually cross the intestinal epithelium barrier to carry insulin into the blood compartment when they are absorbed by portions of the M-cell-free epithelium. Conversely, nanocapsules were highly degraded in M-cell-containing epithelium. This study brings a new input in the debate showing that the fate of biodegradable poly(alkylcyanoacrylate) nanocapsules crossing the intestinal epithelium appeared to differ whether they were absorbed by a portion of epithelium containing M cells or not. It may be interesting to investigate if this effect is related to the difference in local enzymatic content of the respective tissues.

ACKNOWLEDGMENTS

The authors are grateful to Loctite (Dublin, Ireland) for the generous gift of IBCA. They wish to thank Alain Marraud (Ecole Centrale de Paris) for the access to the electron microscope JEOL.

REFERENCES

1. A. Leone-Bay, D. R. Paton, and J. J. Weidner. The development of delivery agents that facilitate the oral absorption of macromolecular drugs. *Med. Res. Rev.* **20**:169–186 (2000).
2. I. Morishita, M. Morishita, K. Takayama, Y. Machida, and T. Nagai. Enteral insulin delivery by microspheres in three different formulations using Eudragit 1100 and S100. *Int. J. Pharm.* **91**:29–37 (1993).
3. E. Mathiowitz, J. S. Jacob, Y. S. Jong, G. P. Carino, D. E. Chichering, P. Chaturverdi, C. A. Santos, K. Vijayaraghavan, S. Montgomery, M. Basset, and C. Morrel. Biologically erodable microspheres as potential oral drug delivery systems. *Nature* **386**: 410–414 (1997).
4. G. Gwinup, A. N. Elias, and E. S. Domurat. Insulin and C-peptide levels following oral administration of insulin in intestinal-enzyme protected capsules. *Gen. Pharm.* **22**:243–246 (1991).
5. N. Hussain, V. Jaitley, and A. T. Florence. Recent advances in the understanding of uptake of microparticulates across the gastrointestinal lymphatics. *Adv. Drug Deliv. Rev.* **50**:107–142 (2001).
6. A. T. Florence. The oral absorption of micro- and nanoparticulates: neither exceptional nor unusual. *Pharm. Res.* **14**:259–266 (1997).
7. F. Delie. Evaluation of nano- and microparticle uptake by the gastrointestinal tract. *Adv. Drug. Deliv. Rev.* **34**:221–233 (1998).
8. D. T. O'Hagan. The intestinal uptake of particles and the implications for drug and antigen delivery. *J. Anat.* **189**:477–482 (1996).
9. J. H. Eldridge, C. J. Hammond, J. A. Meulbroek, J. K. Staas, R. M. Gilley, and T. R. Tice. Controlled vaccine release in the gut-associated lymphoid tissues. 1. Orally administered biodegradable microspheres target the Peyer's patches. *J. Control. Release* **11**:205–214 (1990).
10. P. U. Jani, A. T. Florence, and D. E. McCarthy. Further histological evidence of the gastrointestinal absorption of polystyrene nanospheres in the rat. *Int. J. Pharm.* **84**:245–252 (1992).
11. P. G. Jenkins, K. A. Howard, N. W. Blackhall, N. W. Thomas, S. S. Davis, and D. T. O'Hagan. Microparticulate absorption from the rat intestine. *J. Control. Release* **29**:339–350 (1994).
12. P. U. Jani, D. E. McCarthy, and A. T. Florence. Nanosphere and microsphere uptake via Peyer's patches: observation on the rate of uptake in the rat after a single oral dose. *Int. J. Pharm.* **86**: 239–246 (1992).
13. A. M. Hillery, P. U. Jani, and A. T. Florence. Comparative, quantitative study of lymphoid and non-lymphoid uptake of 60 nm polystyrene particles. *J. Drug Target.* **2**:151–156 (1994).
14. M. Aprahamian, C. Michel, W. Humbert, J. P. Devissaguet, and C. Damgé. Transmucosal passage of polyalkylcyanoacrylate nanocapsules as a new drug carrier in the small intestine. *Biol. Cell* **61**:69–76 (1987).
15. C. Damgé, C. Michel, M. Aprahamian, and P. Couvreur. New approach for oral administration of insulin with polyalkylcyanoacrylate nanocapsules as drug carrier. *Diabetes* **37**:246–251 (1988).
16. C. Michel, M. Aprahamian, L. Defontaine, P. Couvreur, and C. Damgé. The effect of site of administration in the gastrointestinal tract on the absorption of insulin from nanocapsules in diabetic rats. *J. Pharm. Pharmacol.* **43**:1–5 (1991).
17. C. Damgé, D. Hillaire-Buys, R. Puech, A. Holizel, C. Michel, and G. Ribes. Effects of orally administered insulin nanocapsules in normal and diabetic dogs. *Diab. Nutr. Metab.* **8**:3–9 (1995).
18. P. H. Lowe and C. S. Temple. Calcitonin and insulin in isobutylcyanoacrylate nanocapsules: protection against proteases and effect on intestinal absorption in rats. *J. Pharm. Pharmacol.* **46**:547–552 (1994).
19. F. Cournarie, D. Auchere, D. Chevenne, B. Lacour, M. Seiller, and C. Vauthier. Absorption and efficiency of insulin after oral administration of insulin-loaded nanocapsules in diabetic rats. *Int. J. Pharm.* **242**:325–328 (2002).
20. M. Aboubakar, F. Puisieux, P. Couvreur, and C. Vauthier. Physico-chemical characterization of insulin-loaded poly(isobutylcyanoacrylate) nanocapsules obtained by interfacial polymerization. *Int. J. Pharm.* **183**:63–66 (1999).
21. M. Aboubakar, P. Couvreur, H. Pinto-Alphandary, B. Gouritin, B. Lacour, R. Farinotti, F. Puisieux, and C. Vauthier. Insulin-loaded nanocapsules for oral administration: *in vitro* and *in vivo* investigation. *Drug Dev. Res.* **49**:109–117 (2000).
22. S. Mc Clean, E. Prosser, E. Meehan, D. O'Malley, N. Clarke, Z. Ramtoola, and D. Brayden. Binding and uptake of biodegradable poly-DL-lactide micro- and nanoparticles in intestinal epithelia. *Eur. J. Pharm. Sci.* **6**:153–163 (1998).
23. C. Damgé, C. Michel, M. Aprahamian, P. Couvreur, and J. P. Devissaguet. Nanocapsules as carriers for oral peptide delivery. *J. Control. Release* **13**:233–239 (1990).
24. C. Damgé, M. Aprahamian, W. Humbert, and M. Pinget. Ileal uptake of polyalkyl-cyanoacrylate nanocapsules in the rat. *J. Pharm. Pharmacol.* **52**:1049–1056 (2000).
25. L. Szentkuti. Light microscopical observations on luminally administered dyes, dextrans, nanospheres and microspheres in the pre-epithelial mucus gel layer of the rat distal colon. *J. Control. Release* **46**:233–242 (1997).
26. M. Aboubakar, F. Puisieux, P. Couvreur, M. Deyme, and C. Vauthier. Study of the mechanism of insulin encapsulation in poly-(isobutylcyanoacrylate) nanocapsules obtained by interfacial polymerization. *J. Biomed. Material Res.* **47**:568–576 (1999).
27. H. Pinto-Alphandary, O. Balland, M. Laurent, A. Andremont, F. Puisieux, and P. Couvreur. Intracellular visualization of ampicil-

lin-loaded nanoparticles in peritoneal macrophages infected *in vitro* with *Salmonella typhimurium*. *Pharm. Res.* **11**:38–46 (1994).
28. A. Dembri, D. Duchêne, and G. Ponchel. The intestinal mucus protects poly(isobutyl-cyanoacrylate) nanoparticles from enzymatic degradation. *S. T. P. Pharma Sci.* **11**:175–180 (2001).
29. J. Kreuter. Peroral administration of nanoparticles. *Adv. Drug. Deliv. Rev.* **7**:71–86 (1991).
30. C. Pimienta, F. Chouinard, A. Labib, and V. Lenaerts. Effect of various poloxamer coatings on in *vitro* adhesion of isohexylcyanoacrylate nanospheres to rat ileal segments under liquid flow. *Int. J. Pharm.* **80**:1–8 (1992).
31. M. P. Desai, V. Labhasetwar, G. L. Amidon, and R. J. Lévy. Gastrointestinal uptake of biodegradable microparticles: effect of particle size. *Pharm. Res.* **13**:1838–1845 (1996).
32. R. L. Owen and D. K. Bhalla. Cytochemical analysis of alkaline phosphatase and esterase activities and of lectin-binding and anionic sites in rat and mouse Peyer's patch M cells. *Am. J. Anatomy* **168**:199–212 (1983).
33. V. Lenaerts, P. Couvreur, D. Christiaens-Leyh, E. Joiris, M. Roland, B. Rollman, and P. Speiser. Degradation of poly(isobutylcyanoacrylate) nanoparticles. *Biomaterials* **5**:65–68 (1984).
34. J. Kreuter, U. Müller, and K. Munz. Quantitative and microautoradiographic study on mouse intestinal distribution of polycyanoacrylate nanoparticles. *Int. J. Pharm.* **55**:39–45 (1989).